On the Accurate Strain Measurement in Split Hopkinson Tensile Bar Tests

Cheng Chen[(⊠)] and Xudong Qian

Department of Civil and Environmental Engineering, National University of Singapore, 1 Engineering Drive 2, Singapore 117576, Singapore
chencheng@u.nus.edu

Abstract. The Split Hopkinson Tensile Bars (SHTB) are utilized to evaluate the dynamic material property under high strain rates. The one dimensional (1D) wave theory applies to determine the stress and strain of the test specimen. This study adopts the digital image correlation (DIC) technique to measure the full-field deformation along the specimen and compare the strain results with those collected from the strain gauges. The DIC-based strain results reveal nonhomogeneous specimen deformation under the dynamic conditions, and thus provide more accurate strain measurement to establish the stress-strain curve in the SHTB tests.

Keywords: SHTB · 1D wave · DIC · Strain measurement

1 Introduction

The split Hopkinson bar system is the most widely used technique to measure the material property under high strain rates. The experimental work of Hopkinson bar is first investigated by Hopkinson (1872). The Hopkinson bar methods, including tension, pressure, shear, torsion, bending and combined load conditions (Jiang and Vecchio 2009), have been developed in recent decades. The split Hopkinson bar system usually consists of the incident and the transmitter bars, with the specimen sandwiched in between. Although there is no international standard of the split Hopkinson bar tests, several guidelines are summarized by Gray (2012) and Gama et al. (2004), recommending general setup such as the bar configuration and the strain gauge position. Under their recommendations, common issues such as the oscillation and dispersion (Gu et al. 2016) are alleviated in the impact tests, which facilitates the application of classical 1D wave theory (Kolsky 1949) and enhances the accuracy of the stress-strain results.

Recent development on digital image correlation (DIC) techniques (Pan 2011) has provided an alternative method for the non-contact strain measurement. DIC is a computer-vision based technique which allows full-field deformation tracing. Pierron et al. (2011) utilize the high-speed camera to examine the bending wave under a three-point-bending split Hopkinson bar test and discuss the inertial effects during the impact. Gilat et al. (2009) adopt the 3D-DIC technique to analyze the full-field strain under different strain rates. The DIC results reveal the deformation difference of the copper

specimens in compressive and tensile split Hopkinson bar tests. Verleysen et al. (2008) investigate the geometry effects on the strain accuracy by changing the gauge area and the transition zone size in the dog-bone specimens. An optical measurement is utilized to compare with the results collected by the strain gauges. Their experimental results indicate that specimens with higher effective length-to-width ratio (≥ 1) yield better strains consistency between the optical and traditional measurement. Rusinek et al. (2008) optimize the specimen dimension through numerical analysis. The authors also demonstrate the importance of the transition zone size to the accuracy of the stress-strain curves.

This paper aims to establish the stress-strain curve data of the aluminum materials under different strain rates and investigate the strain accuracy through the non-contact DIC method. The servo-hydraulic machine is utilized for the quasi-static test while the split Hopkinson tensile bar (SHTB) is used for the high-strain-rate tests. The high-speed camera records the images during the impact tests and enables the full-field deformation measurement on the specimen gauge area. Strain results from the strain gauge method are compared with the DIC measurement to investigate the dynamic effects on the strain measurement.

2 Methodology

The split Hopkinson tensile bar consists of the striking bar, gas gun, the incident and the transmitter bars. Figure 1 shows the SHTB system used in the current study. The specimen is placed between the incident and the transmit bars. Strain gauges are mounted in the bars to collect the strain values during the impact tests.
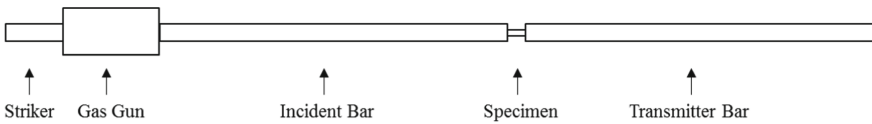

Fig. 1. SHTB system

The 1D wave theory applies to determine the specimen stress and strain from the bar data (Kolsky 1949). The 1D wave theory assumes that the bars are linear and dispersion-free, while the specimen experiences negligible inertial effects (Gray 2000). The 1D wave propagation follows the fundamental equations,

$$\frac{\partial^2 u}{\partial x^2} = \frac{1}{c^2}\frac{\partial^2 u}{\partial t^2} \tag{1}$$

$$\dot{u}_I = -c(\varepsilon_I - \varepsilon_R) \tag{2}$$

$$\dot{u}_T = -c\varepsilon_T \tag{3}$$

where u is the displacement, $\dot{u}$ is the displacement rate, x denotes the wave propagation direction, c represents the wave propagation velocity, t refers to the time and ε is the

strain. The subscript I, R, T denotes the incident, reflect and transmit waves. Based on the stress equilibrium between the incident and the transmitter bars, the strain and stress of the specimen derive as,

$$\dot{\varepsilon} = 2c\varepsilon_R/L_s \tag{4}$$

$$\varepsilon = 2c/L_s \int_0^t \varepsilon_R dt \tag{5}$$

$$\sigma = EA\varepsilon_T/A_s \tag{6}$$

where $\dot{\varepsilon}$ is the strain rate, L_s and A_S are the specimen gauge length and cross-section area. E and A are the elastic modulus and the cross-section area of the Hopkinson bars. σ indicates the specimen stress. The classical 1D wave theory measures the specimen stress and strain from the strain gauge data, and is widely adopted for the SHTB tests (Huh et al. 2002; Tucker et al. 2010).

3 Experimental Tests

3.1 Quasi-static Test

The quasi-static tests are conducted under a servo-hydraulic machine in the Structural Engineering Laboratory at National University of Singapore. The specimens are made of aluminium 5083. Figure 2a shows the configuration of the aluminium specimen. The specimen has a total length of 56mm and an effective gauge length of 4 mm. The width in the gauge area is 4 mm while the transition zone has a radius of 7.5 mm. The specimen thickness is 1mm. The quasi-static test shows a yielding stress of 258 MPa and an elastic modulus of 70 GPa for the aluminium 5083 material. The engineering stress-strain curve from the quasi-static tests is plotted in Fig. 2b.
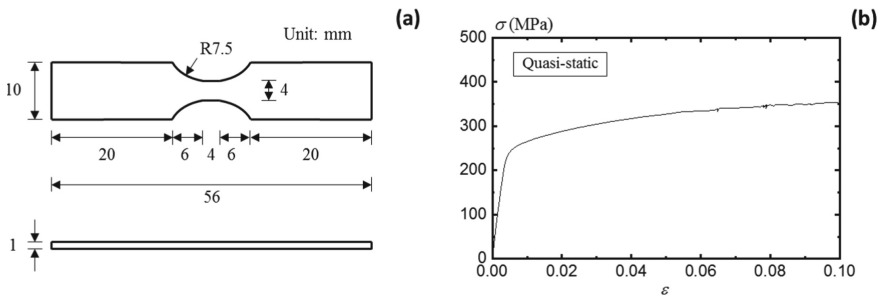

Fig. 2. (a) Specimen configuration; (b) Quasi-static stress-strain curve

3.2 SHTB Test

Figure 3 presents the experimental setup for the SHTB tests. The tests are carried out in the Impact Laboratory of National University of Singapore. The high-speed camera is utilized to record the specimen deformation during the impact tests. The image plane is parallel placed with the specimen to reduce the correlation error. The camera has a resolution of 128 × 64 pixels with a frame rate of 300000 frames per second. The actual length to pixel ratio is 0.08 mm/pixel for the current specimen, which is similar to the dynamic DIC resolution in Reu and Miller (2008) and Pop et al. (2011). The illumination creates the contrast for the image correlation. The specimen has the same dimension as the quasi-static coupon specimen (Fig. 2) to ensure the direct comparison of the material response under different loading conditions. The specimen surface is covered with speckles for the image correlation. Two additional bolts are fabricated at the grip end of the specimen to connect with the Hopkinson bars. The strain rates range from 500/s to 3000/s for the SHTB tests in the current study.
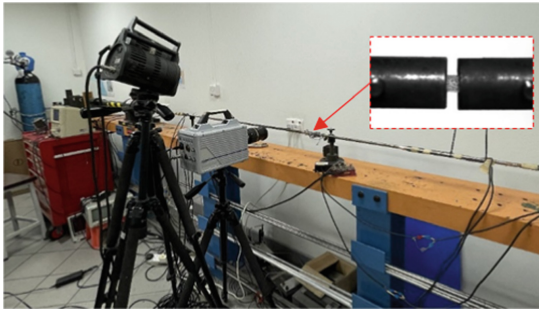

Fig. 3. SHTB test setup

Figure 4a illustrates the strain results from the incident and transmitter bars at the strain rate of 2000/s. Figure 4b calculates the stress-strain curve under impact load following Eqs. (1–6) and the results are compared with the quasi-static results. Although the material indicates clear signs of yielding, hardening and necking stages during the impact test, the strain results are not reliable considering the critical discrepancy between the impact and the static test results. In contrast to the material response under quasi-static condition, the impact test shows a severely deviated initial slope, which leads to an underestimated elastic modulus at high strain rates. The elastic modulus is only around 3 GPa compared with the 70 GPa in the quasi-static test. Several researchers have also reported similar phenomenon and attributed the underestimation of the elastic modulus to the transition zone size (Verleysen et al. 2008) and the grip effect (Huh et al. 2002). In light of the inaccuracy of strain from the traditional strain gauge measurement, the DIC method is further applied to evaluate the strain abnormality in the SHTB tests.

To investigate the strain variation along the specimen, three virtual extensometers (VE) are defined in the gauge area, with 1–3 mm length respectively. Furthermore, the middle point is also selected to extract the pointwise strain values (Fig. 5a). Figure 5b presents the horizontal displacement at 150 μs after the impact. x denotes the elongation
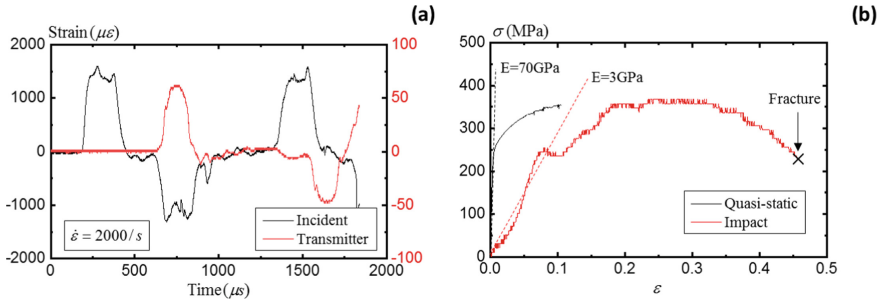
Fig. 4. (a) Strain gauge results; (b) Stress-strain curves comparison

direction. The horizontal displacement indicates non-uniform distribution within the gauge area, as the deformation gradients varies along the *x* direction.
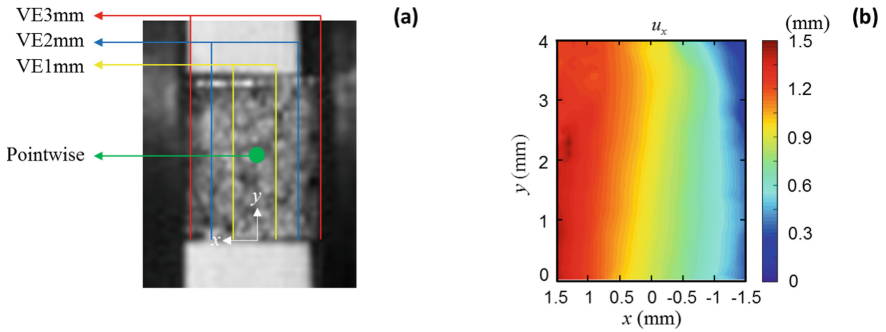

Fig. 5. (a) Definition of virtual extensometer; (b) DIC-measured displacement

Figure 6a summarizes the elongation measured by different virtual extensometers (Fig. 5a) using the DIC method. The bar results are also included as a comparison. Apparently a critical difference exists between the displacement from the bar end and the specimen. This reveals the overestimation of the specimen displacement using the bar data. The discrepancy originates from the grip connection between the bar and the specimen. Figure 6b further calculates the strain results from the bar data and the DIC measurement. The DIC results demonstrate the over-prediction of the strain values from the bar ends, especially at the start of the impact. This explains the underestimation of the elastic modulus in Fig. 4b.

On the other hand, the strain results based on different VE lengths are also different inside the gauge area. Figure 6b shows that the strains decrease with the VE length in the initial 150 μs time after the impact, which reflects the nonhomogeneous deformation along the gauge area in Fig. 5b. This non-homogeneity marks the critical characteristic of the specimen deformation under impact loads. Unlike the quasi-static condition where the gauge area observes similar strain patterns, the location of the VE affects the dynamic strain results. A local 1 mm VE yields similar strain results compared with the pointwise strain measurement from the DIC field. Since the fracture occurs in the middle of the

specimen, the strain results closer to the middle of the gauge region represent more accurate material strains for the impact tests. The pointwise strains increase dramatically after 150 μs due to the localized necking before the fracture occurs. This study focus on the material response before the necking and exclude the strain data after 150 μs.
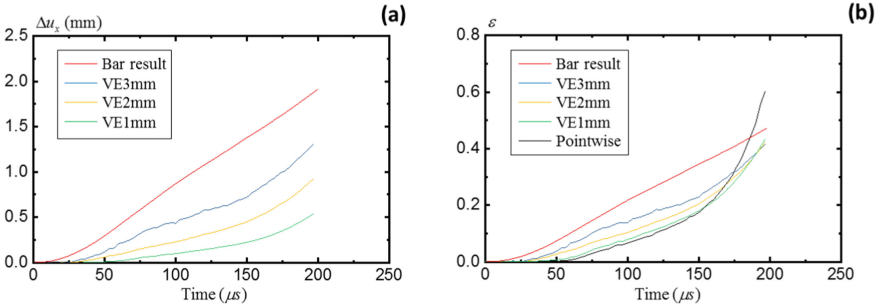
Fig. 6. (a) Comparison of the elongations; (b) Comparison of the strains

Since the strain results from the bar measurement is not able to represent the actual specimen strain accurately, the DIC-based strain results are utilized as the actual strain of the specimen. Figure 7a replace the strains in Fig. 4b with the DIC-based pointwise strain results while retaining the stress values. The modified strain-stress curve coincides with the quasi-static test in the initial elastic stage. The elastic modulus is close to 70 GPa in the DIC-modified curve. The modified results demonstrate the accuracy of the DIC strain measurement. The aluminium material shows slightly increased strength under impact loading, although only a 5% difference is observed compared to the quasi-static results.
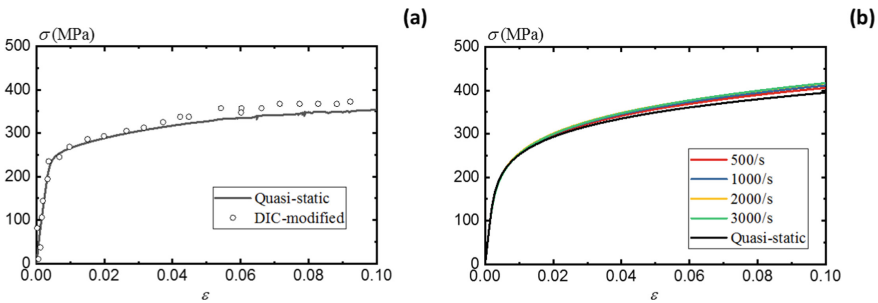
Fig. 7. (a) DIC-modified stress-strain curve; (b) True stress-strain curves

Following the same procedures, Fig. 7b summarizes the DIC-modified true stress–strain results under various strain rates from 500 to 3000/s. The stress-strain data are fitted using the Ramberg-Osgood expression (Ramberg and Osgood 1943). The Aluminium 5083 show relatively low rate-dependence under high strain rates. Although the material demonstrates slightly enhanced strength under impact conditions, the difference

under strain rates of 500/s and 3000/s is not distinguishable. The rate-insensitivity of Aluminium materials are also reported by (Chen et al. 2009). The strain modification by the DIC method effectively correct the strain overestimation from the bar results. The full-field DIC results demonstrate the nonhomogeneous deformation and the pointwise strain results represents the accurate specimen strain during the impact tests.

4 Conclusions

This paper investigates the strain discrepancy between the bar results and the specimen using the DIC method and discusses the strain rate effects on the Aluminum 5083 material. The DIC results reveal the non-homogeneity of deformation in the gauge area and provide more accurate strain measurement for the split Hopkinson tensile bar tests. The strain results measured by the strain gauges on the bars significantly overestimate the specimen strain and lead to critically biased elastic modulus. The DIC-modified strain results achieve better agreement with the quasi-static results at the elastic stage. Therefore, the DIC method is a preferred approach to obtain the accurate strain results for impact tests.

The DIC-modified stress-strain curves show that the Aluminum 5083 material is insensitive to the strain rate. The material strength under 3000/s strain rate is similar to that under 500/s strain rate, and both results only have a 5% increase compare to the quasi-static material property.

References

Chen, Y., et al.: Stress-strain behaviour of aluminium alloys at a wide range of strain rates. Int. J. Solids Struct. **46**(21), 3825–3835 (2009). https://doi.org/10.1016/j.ijsolstr.2009.07.013

Gama, B.A., Lopatnikov, S.L., Gillespie, J.W.: Hopkinson bar experimental technique: a critical review. Appl. Mech. Rev. **57**(1–6), 223–250 (2004). https://doi.org/10.1115/1.1704626

Gilat, A., Schmidt, T.E., Walker, A.L.: Full field strain measurement in compression and tensile split Hopkinson bar experiments. Exp. Mech. **49**(2), 291–302 (2009). https://doi.org/10.1007/s11340-008-9157-x

Gray, G.T. (Rusty): High-strain-rate testing of materials: the Split-Hopkinson pressure bar. Characterization Mater. (2012). https://doi.org/10.1002/0471266965.com023.pub2

Gray III, G.T.: Classic split Hopkinson pressure bar testing. ASM handbook. Mech. Test. Eval. **8**, 462–476 (2000)

Gu, X., et al.: Wave dispersion analysis and simulation method for concrete SHPB test in peridynamics. Eng. Fracture Mech. **160**, 124–137 (2016)

Hopkinson, J.: On the rupture of iron wire by a blow. Proc. Literary Philos. Soc. Manchester **1**, 40–45 (1872)

Huh, H., Kang, W.J., Han, S.S.: A tension split Hopkinson bar for investigating the dynamic behavior of sheet metals. Exp. Mech. **42**(1), 8–17 (2002). https://doi.org/10.1177/0018512002042001784

Jiang, F., Vecchio, K.S.: Hopkinson bar loaded fracture experimental technique: a critical review of dynamic fracture toughness tests. Appl. Mech. Rev. **62**(6), 1–39 (2009). https://doi.org/10.1115/1.3124647

Kolsky, H.: An investigation of the mechanical properties of materials at very high rates of loading. In: Proceedings of the Physical Society. Section B, vol. 62, issue 11, p. 676. IOP Publishing (1949)

Pan, B.: Recent progress in digital image correlation. Exp. Mech. **51**(7), 1223–1235 (2011)

Pierron, F., Sutton, M.A., Tiwari, V.: Ultra high speed DIC and virtual fields method analysis of a three point bending impact test on an aluminium bar. Exp. Mech. **51**(4), 537–563 (2011). https://doi.org/10.1007/s11340-010-9402-y

Pop, O., et al.: Identification algorithm for fracture parameters by combining DIC and FEM approaches. Int. J. Fract. **170**(2), 101–114 (2011). https://doi.org/10.1007/s10704-011-9605-y

Ramberg, W., Osgood, W.R.: Description of Stress-Strain Curves by Three Parameters (1943)

Reu, P.L., Miller, T.J.: The application of high-speed digital image correlation. J. Strain Anal. Eng. Des. **43**(8), 673–688 (2008). https://doi.org/10.1243/03093247JSA414

Rusinek, A., et al.: Dynamic behaviour of high-strength sheet steel in dynamic tension: experimental and numerical analyses. J. Strain Anal. Eng. Des. **43**(1), 37–53 (2008). https://doi.org/10.1243/03093247JSA320

Tucker, M.T., et al.: The effect of varying strain rates and stress states on the plasticity, damage, and fracture of aluminum alloys. Mech. Mater. **42**(10), 895–907 (2010). https://doi.org/10.1016/j.mechmat.2010.07.003

Verleysen, P., et al.: Influence of specimen geometry on split hopkinson tensile bar tests on sheet materials. Exp. Mech. **48**(5), 587–598 (2008). https://doi.org/10.1007/s11340-008-9149-x